How release of phosphate from mammalian F_1-ATPase generates a rotary substep

John V. Bason[a], Martin G. Montgomery[a], Andrew G. W. Leslie[b], and John E. Walker[a,1]

[a]Medical Research Council Mitochondrial Biology Unit, Cambridge Biomedical Campus, Hills Road, Cambridge CB2 0XY, United Kingdom; and [b]Medical Research Council Laboratory of Molecular Biology, Cambridge Biomedical Campus, Cambridge CB2 0QH, United Kingdom

Contributed by John E. Walker, April 2, 2015 (sent for review March 6, 2015; reviewed by Hiroyuki Noji and Dale B. Wigley)

The rotation of the central stalk of F_1-ATPase is driven by energy derived from the sequential binding of an ATP molecule to its three catalytic sites and the release of the products of hydrolysis. In human F_1-ATPase, each 360° rotation consists of three 120° steps composed of substeps of about 65°, 25°, and 30°, with intervening ATP binding, phosphate release, and catalytic dwells, respectively. The F_1-ATPase inhibitor protein, IF_1, halts the rotary cycle at the catalytic dwell. The human and bovine enzymes are essentially identical, and the structure of bovine F_1-ATPase inhibited by IF_1 represents the catalytic dwell state. Another structure, described here, of bovine F_1-ATPase inhibited by an ATP analog and the phosphate analog, thiophosphate, represents the phosphate binding dwell. Thiophosphate is bound to a site in the $\alpha_E\beta_E$-catalytic interface, whereas in F_1-ATPase inhibited with IF_1, the equivalent site is changed subtly and the enzyme is incapable of binding thiophosphate. These two structures provide a molecular mechanism of how phosphate release generates a rotary substep as follows. In the active enzyme, phosphate release from the β_E-subunit is accompanied by a rearrangement of the structure of its binding site that prevents released phosphate from rebinding. The associated extrusion of a loop in the β_E-subunit disrupts interactions in the $\alpha_E\beta_E$-catalytic interface and opens it to its fullest extent. Other rearrangements disrupt interactions between the γ-subunit and the C-terminal domain of the α_E-subunit. To restore most of these interactions, and to make compensatory new ones, the γ-subunit rotates through 25°–30°.

mitochondria | ATP synthase | phosphate release | rotary substep

The ATP synthase in bovine mitochondria is a membrane-bound protein assembly of about 30 polypeptides of 18 different kinds with a combined molecular mass of about 650 kDa (1, 2). They are organized into a membrane extrinsic globular F_1-catalytic domain and a membrane intrinsic domain joined together by central and peripheral stalks. The F_1-domain is an assembly of three α-subunits and three β-subunits arranged in alternation in a spherical complex around an α-helical structure in the γ-subunit (3), and the three catalytic sites of the enzyme lie at three of the six interfaces between the α- and β-subunits. The γ-subunit extends from the $\alpha_3\beta_3$-spherical structure to the membrane domain of the enzyme, where it is augmented by the δ- and ε-subunits in the region of contact with a membrane-embedded ring of eight c-subunits (4). The γ-, δ-, and ε-subunits form the central stalk, and together with the c-ring, it constitutes the rotor of the enzyme. During ATP synthesis, the rotor turns clockwise as viewed from the membrane domain of the complex. Rotation is driven by the potential energy of a transmembrane proton motive force generated by respiration, and the rotor transmits energy into the F_1-domain, bringing about the conformational changes in the three catalytic sites that are required to produce ATP from ADP and phosphate.

The F_1-domain has been studied extensively in isolation from the rest of the enzyme complex. It is a globular assembly that functions as an ATP hydrolase, and many structural studies of the eukaryotic F_1-ATPase (3–11) and biophysical studies of bacterial enzymes (12–14) have illuminated how the hydrolysis of ATP at its three catalytic sites drives the anticlockwise rotation of the central stalk as viewed from the membrane domain of the intact enzyme. The catalytic sites are formed predominantly from residues in the β-subunits plus an essential contribution from a residue known as the "arginine finger" at position 373 in the adjacent α-subunits (15). During a 360° rotary cycle, each β-subunit passes through three states corresponding to the β_E-, β_{TP}-, and β_{DP}-subunits observed in the "reference" structure of the enzyme, where E, TP, and DP correspond to the unoccupied, or "empty," ATP binding and ADP binding conformations respectively (3).

The hydrolysis of ATP by F_1-ATPase from mitochondria, but not from bacteria or chloroplasts, can be inhibited by the natural inhibitor of F_1-ATPase, IF_1 (16). Bovine IF_1 is 84 aa long (17), and the active form is a homodimer held together by an antiparallel coiled-coil of α-helices from residues 49–81 (18). Its N-terminal region from residues 1–45 provides the inhibitory part of the protein. In the free inhibitor, this region is intrinsically disordered (19), and it becomes structured progressively as it binds to the enzyme (20) and inhibits ATP hydrolysis. A monomeric derivative of bovine IF_1 containing residues 1–60 is also an effective inhibitor, and it was found to be bound to the C-terminal domains of both the α- and β-subunits in one, two, or all three catalytic interfaces of F_1-ATPase (21, 22).

The rotation of the central stalk of F_1-ATPase has been studied by direct observation of the tethered enzyme. In the F_1-ATPase from the *Bacillus stearothermophilus* strain PS3, each 360° rotary cycle has been resolved at high concentrations of ATP (2 mM) into three 120° steps (14). The three intervening pauses are referred to as the "catalytic dwells," where the enzyme is considered to be poised to carry out, or to be carrying out, the

Significance

ATP, the fuel of life, is produced in the mitochondria of living cells by a molecular machine consisting of two motors linked by a rotor. One motor generates rotation by consuming energy derived from sugars and fats in foodstuffs; the other uses energy transmitted by the rotor to synthesize ATP molecules from their building blocks, ADP and phosphate. The synthetic motor can be uncoupled from the machine, and its rotary action can be studied by driving the motor backward with energy from ATP, releasing ADP and phosphate in the process. Each cycle has three 120° steps, each made of substeps of 65°, 25°, and 30° in humans. We have explained how release of phosphate from the machine generates the 25° rotary substep.

Author contributions: J.V.B. and J.E.W. designed research; J.V.B. and M.G.M. performed research; J.V.B., M.G.M., A.G.W.L., and J.E.W. analyzed data; J.V.B., M.G.M., A.G.W.L., and J.E.W. wrote the paper; and J.E.W. supervised the project.

Reviewers: H.N., University of Tokyo; and D.B.W., Institute of Cancer Research.

The authors declare no conflict of interest.

Freely available online through the PNAS open access option.

Data deposition: The atomic coordinates and structure factors have been deposited in the Protein Data Bank, www.pdb.org (PDB ID codes 4YXW and 4Z1M).

[1]To whom correspondence should be addressed. Email: walker@mrc-mbu.cam.ac.uk.

This article contains supporting information online at www.pnas.org/lookup/suppl/doi:10.1073/pnas.1506465112/-/DCSupplemental.

BIOCHEMISTRY

hydrolysis of ATP. At lower concentrations of ATP (2 μM), a second pause can be observed 40° after the catalytic dwell. It is known as the "ATP binding dwell," where the enzyme is awaiting the binding of the substrate, ATP (14). The rotary 360° cycle of the human F_1-ATPase also contains three catalytic dwells separated by 120°, and 30° after each catalytic dwell, three ATP binding dwells (23). Unlike the bacterial enzyme, both dwells in the human enzyme can be observed at both high (4 mM) and low (50 μM) concentrations of ATP. Inhibition of the human enzyme with human IF_1 halts the rotary cycle at a position corresponding to the catalytic dwell (23). Thus, structures of the closely related bovine enzyme inhibited by bovine IF_1 (21, 22) can be considered to be structural representations of the catalytic dwell. Moreover, upon addition of the ATP analog adenosine 5′-(β,γ-imido)triphosphate (AMP-PNP) and the phosphate analog monothiophosphate (referred to as "thiophosphate"), the rotating human enzyme stalls at an additional intermediate position 25° before the catalytic dwell (23). Although this intermediate stall position has been referred to as the "phosphate release dwell," it differs from the catalytic and ATP binding dwells in that it has not been observed during each 120° step in an active catalytic cycle, and it is manifest only when rotation of the enzyme has been stopped with the inhibitors AMP-PNP and thiophosphate. It is reasonable to assume that this state corresponds to a point in catalysis after the cleavage of the β-γ phosphate bond of ATP, where phosphate is about to be released.

Therefore, as described here, we have determined a structure of bovine F_1-ATPase with crystals grown in the presence of AMP-PNP and thiophosphate. To ascertain whether the bovine F_1-ATPase inhibited with IF_1 is capable of binding thiophosphate, we have also redetermined its structure with crystals of the inhibited complex grown in the presence of thiophosphate. Because these structures correspond to the prephosphate release and the catalytic dwell states of the enzyme, respectively, they provide the basis of a molecular explanation of the mode of binding of phosphate to F_1-ATPase at the attendant dwell, and how the subsequent release of phosphate from the enzyme is coupled to the generation of the 25° rotary substep between the phosphate release and catalytic dwells.

Results

Structure Determination. The structures of the two bovine F_1-ATPase complexes, F_1-ATPase inhibited with AMP-PNP and thiophosphate (known as F_1-ThioP) and F_1-ATPase inhibited with I1-60His-K39A and ATP (*Materials and Methods*) and the crystals grown in the presence of thiophosphate (known as F_1-I_3-ThioP), were determined by molecular replacement with data to 3.1 Å and 3.3 Å resolution, respectively. The asymmetric units of both crystals contain one F_1-ATPase, and in the case of F_1-I_3-ThioP, three inhibitor proteins bound to the enzyme in catalytic interfaces. The data processing and refinement statistics are summarized in Table S1. The final model of F_1-ThioP contains the following residues: α_E, 22–510; α_{TP}, 23–401 and 410–510; α_{DP}, 23–510; β_E, 9–387 and 396–474; β_{TP}, 9–474; β_{DP}, 9–475; γ, 1–49, 67–96, 107–148, 159–173, and 196–272; δ, 15–53 and 57–145; and ε, 1–47. An Mg-AMP-PNP complex is bound to the nucleotide binding sites in each of the three noncatalytic α-subunits and in the catalytic β_{DP}- and β_{TP}-subunits, and a thiophosphate ion, but no nucleotide, is bound to the β_E-subunit. Likewise the final model of F_1-I_3-ThioP contains α_E, 24–510; α_{TP}, 16–402 and 411–510; α_{DP}, 23–404 and 410–510; β_E, 8–477; β_{TP}, 9–477; β_{DP}, 9–477; γ, 1–44, 73–91, 108–153, 164–173, and 205–272; I1-60_E, 29–50; I1-60_{TP}, 23–50; and I1-60_{DP}, 10–50. However, the inhibited complex was formed by inhibiting the active F_1-ATPase with IF_1, and therefore in this structure, the nucleotide binding site in each of the three noncatalytic α-subunits is occupied by an Mg-ATP complex, both the β_{DP}- and β_{TP}-subunits contain a bound Mg-ADP moiety, and neither a nucleotide nor a thiophosphate ion is bound to the β_E-subunit. Attempts to crystallize bovine F_1-ATPase in the presence of phosphate and nucleotides were unsuccessful because the protein aggregated and precipitated.

Structure of the Bovine F_1–ThioP Complex. In many respects, the structure of F_1-ThioP (Fig. 1) is similar to previous structures of bovine F_1-ATPase. It resembles especially the ground state structure, where the β_E-subunit is fully open and unoccupied by either substrate or hydrolysis products (6) and the superimposed structures have an rmsd of 0.6 Å for all atoms. In the initial refinement of the model of F_1-ThioP, a strong positive electron difference density peak (>8σ) was revealed in the region of the catalytic site of the β_E-subunit. Because the crystals were grown in the presence of thiophosphate, and in the absence of phosphate or sulfate, this density probably represents a bound thiophosphate ion, and its shape is consistent with a phosphorous atom, with three equivalent oxygen atoms and a sulfur atom at the fourth apex of an asymmetric tetrahedron facing toward β_E-R189 (Fig. 2*A*). Its three negatively charged oxygen atoms form ionic interactions with the guanidinium of β_E-R260, the amido moiety of β_E-N257, and the ε-amino group of β_E-K162, and its sulfur atom

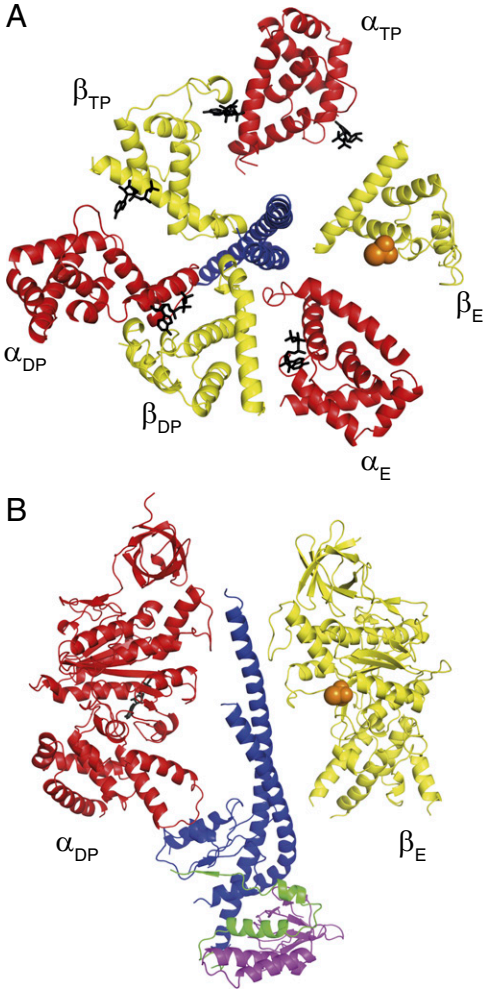

Fig. 1. Structure of the bovine F_1-ThioP complex. Cross-sectional views of the F_1-ATPase from above and toward the membrane domain of the intact ATP synthase of the C-terminal domains of the α- and β-subunits (residues 380–510 and 364–474, respectively), arranged alternately around the γ-subunit (residues 1–47 and 206–270) (*A*) and from the side showing the α_{DP}-subunit; the γ-, δ-, and ε-subunits; and the β_E-subunit (*B*). The α-, β-, γ-, δ-, and ε-subunits are colored red, yellow, blue, magenta, and green, respectively. Bound nucleotides and a thiophosphate ion are colored black and orange, respectively.

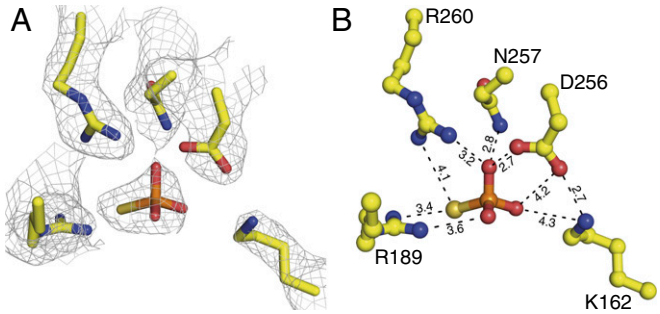

Fig. 2. Thiophosphate bound to the β_E-subunit of the F_1-ThioP complex. (*A*) Electron density of the $2F_O$-F_C map of the thiophosphate binding site (contour level = 1.0 σ). The electron density (gray mesh) extends for a radius of 1.6 Å around the residues of the binding site. (*B*) Side chains of residues contributing to the thiophosphate binding site and their distances (in angstroms) from the bound thiophosphate. The side chains of residues of the β_E-subunit and the thiophosphate are colored yellow and orange, respectively. Oxygen, nitrogen, and sulfur atoms are colored red, blue, and gold, respectively.

makes a fourth ionic interaction with the guanidinium of residue β_E-R189 (Fig. 2*B*). In addition, there is a hydrogen bond between a thiophosphate oxygen atom, which is probably protonated, and the carboxylate group of β_E-D256.

Structure of the Bovine F_1–I_3–ThioP Complex. The structure of F_1-I_3-ThioP (Fig. S1) is essentially identical to the structure of F_1-(I1-60His K39A)$_3$ (21); the rmsd for all atoms of the two superimposed structures is 0.4 Å. Both complexes consist of F_1-ATPase with three inhibitor proteins bound to the C-terminal α-helical domains of α- and β-subunits in the $\alpha_E\beta_E$-, $\alpha_{TP}\beta_{TP}$-, and $\alpha_{DP}\beta_{DP}$-catalytic interfaces of the enzyme. As observed previously (21), in both complexes, the extent of the secondary structure of the inhibitor proteins resolved at each catalytic interface differs (Fig. S1). The least extensively defined inhibitor is the one at the $\alpha_E\beta_E$-catalytic interface, where residues 29–50 were resolved. A more extensive section of the inhibitor protein from residues 23–50 was resolved at the $\alpha_{TP}\beta_{TP}$-catalytic interface, and the inhibitor at the $\alpha_{DP}\beta_{DP}$-catalytic interface had the most extensive secondary structure, extending from residues 10–50. There was no evidence of a thiophosphate ion bound to the β_E-subunit of F_1-I_3-ThioP, and no bound anion (phosphate or sulfate) was found previously bound in the β_E-subunit of F_1-(I1-60His K39A)$_3$ (21).

Discussion

Phosphate Binding Sites in F_1-ATPase. The thiophosphate binding site in F_1-ThioP is equivalent to the site where sulfate has been observed to be bound previously in one of the three F_1-ATPase complexes ("molecule" II) in the asymmetric unit of crystals of the ground state structure of F_1-ATPase from *Saccharomyces cerevisiae* (8) (Fig. S2) and in a structure of bovine F_1-ATPase inactivated covalently with dicyclohexylcarbodiimide (known as F_1-DCCD) (7) (Fig. S3*A*). In the structure of bovine F_1-ATPase inhibited with ADP and aluminum fluoride (known as F_1-AlF_4), ADP and sulfate are bound to the half-closed β_E-subunit, with the sulfate occupying the same position as the sulfate in F_1-DCCD (15) (Fig. S3*B*). In all of the other structures of bovine F_1-ATPase, there is no evidence for either phosphate or sulfate being bound at a site equivalent to the site where thiophosphate is bound in F_1-ThioP. However, in the structures of bovine F_1-ATPase in the ground state (3), in the enzyme inhibited with beryllium fluoride (9) or azide (5), and in the complex with F_1-ATPase and the peripheral stalk subcomplex (10), electron density in the β_E-subunit adjacent to the phosphate binding loop (P-loop), was interpreted as either a phosphate or a sulfate ion (Fig. S3*C*). The P-loop is a conserved feature of many NTPases, and is so-named because it interacts with phosphate moieties of bound NTP or NDP molecules (24). In these structures of bovine F_1-ATPase, the anion binding site in the β_E-P-loop is about 8 Å from where the γ-phosphate of the substrate ATP is bound in the catalytically active β_{DP}-subunit, and from where phosphate is presumably released following scission of the bond between the β- and γ-phosphates. Currently, there is no experimental evidence supporting the involvement of a phosphate ion bound in the vicinity of the β_E-P-loop of F_1-ATPase in the mechanism of hydrolysis of ATP (8).

Changes in the Phosphate Binding Site in F_1-ThioP and F_1-I_3-ThioP. In the structure of F_1-I_3-ThioP, the site in the β_E-subunit that is equivalent to the thiophosphate binding site in the F_1-ThioP complex differs subtly from that site. In F_1-ThioP, the thiophosphate interacts with β_E-K162, β_E-R189, β_E-D256, β_E-N257, and β_E-R260 (Fig. 2), and residue β_E-E188 is positioned directly above the bound thiophosphate in a loop (residues 187–189) at the $\alpha_E\beta_E$-interface (Fig. 3*A*). In contrast, in F_1-I_3-ThioP, the side chain of β_E-E188 points "downward" (Fig. 3*B*); its carboxylate group has moved by 7 Å and now occupies the position occupied by the guanidinium of β_E-R260 in F_1-Thio-P (Fig. 3*A*). In addition, in F_1-I_3-ThioP, both β_E-R189 and β_E-R260 have moved away from the thiophosphate binding site by 1.5–2.0 Å relative to their positions in F_1-ThioP (Fig. 3*B*). This rearrangement has prevented thiophosphate from binding to F_1-I_3-ThioP, and is associated with a concerted movement of residues β_E-Q221, β_E-N223, and β_E-E188, and the extrusion of the loop (residues β_E-G187 to β_E-R189), toward the $\alpha_E\beta_E$-interface (Fig. 4 and Movie S1). As a result, overall, the $\alpha_E\beta_E$-interface is more open in F_1-I_3-ThioP than in F_1-ThioP (accompanying identification of structural features is provided in Fig. S4 and Movie S2), although residues α_E130-α_E136 in F_1-I_3-ThioP are closer to the β_E-subunit than in F_1-ThioP. The rmsd for all atoms for the $\alpha_E\beta_E$ dimers of the F_1-ThioP and F_1-I_3-ThioP complexes is 2.1 Å.

This interpretation of the differences in the phosphate binding site in F_1-ThioP and F_1-I_3-ThioP is supported by the structures of bovine F_1-ATPase inhibited by two or three copies of the inhibitor protein (21). In all three structures, the side chain of β_E-E188 is in the "downward" conformation. However, in the historically first determined structure of bovine F_1-ATPase inhibited with residues 1–60 of bovine IF_1 (22), the concerted side-chain movements of residues β_E-E188, β_E-R260, β_E-Q221, and β_E-N223 were not observed. This difference may be accounted for by increased crystal lattice contacts arising from the controlled dehydration and shrinkage of the unit cell of the crystals of this particular complex before collection of X-ray diffraction data. This dehydration procedure was not used in any of the subsequent structure determinations of F_1-inhibitor protein complexes.

Changes in the γ-Subunit in F_1-ThioP and F_1-I_3-ThioP. In the structures of F_1-ThioP and the ground state structure of F_1-ATPase (6), the γ-subunit is found in the same position. In contrast in F_1-I_3-ThioP and all of the other structures of F_1-ATPase with a bound inhibitor protein, including the first structure of the F_1-inhibitor complex (22), the γ-subunits are in a different common position where, relative to F_1-ThioP, the subunit has rotated by ∼30° in an anticlockwise direction as viewed from the membrane domain of the intact ATP synthase (Table S2). This rotation is accompanied by changes in the mode of interaction of the γ-subunit with the α- and β-subunits close to where the γ-subunit emerges from the $\alpha_3\beta_3$-domain (Tables S3 and S4; see below). However, other interactions, between the γ-subunit and the "bearing" region in the "crown" domain involving the N-terminal regions of α- and β-subunits are unchanged.

Release of Phosphate and Generation of the 25° Rotary Substep in Mammalian F_1-ATPase. The sequences of human and bovine α-, β-, and γ-subunits are 99%, 99%, and 93% identical, respectively. Thus, bovine F_1-ThioP and bovine F_1-I_3-ThioP are structural

BIOCHEMISTRY

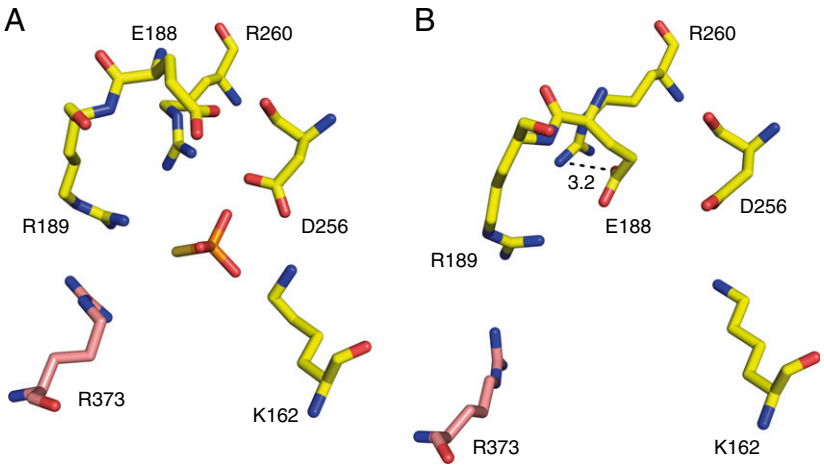

Fig. 3. Comparison of the structures of the thiophosphate binding site in the F_1-ThioP complex and of the equivalent sites in complexes of bovine F_1-ATPase inhibited with the natural inhibitor protein, IF_1. F_1-ThioP (*A*) and F_1-I_3-ThioP (*B*) are shown. The residues of the surrounding β_E-subunit, the Arg finger residue α_ER373, and the thiophosphate are colored yellow, pink, and orange, respectively. Oxygen, nitrogen, and sulfur atoms are colored red, blue, and gold, respectively. The distance of the salt bridge interaction between β_E-E188 and β_E-R260 is shown in angstroms.

representations of F_1-ATPase in the phosphate release dwell and the postphosphate release states of bovine and human F_1-ATPases, respectively, and they provide a molecular mechanism of the coupling of phosphate release to the 25° rotary substep. The observation that the γ-subunit in the structure of F_1-I_3-ThioP and related structures is 30° from its position in F_1-ThioP (as viewed from the membrane domain of the intact ATP synthase; Table S2) is consistent with this interpretation, and the 30° step observed in the structures is considered to be equivalent to the 25° substep observed in rotational experiments.

In this mechanism, the release of phosphate from the β_E-catalytic site is accompanied by the movement of the side chains of β_E-E188, β_E-R189, and β_E-R260; the Glu toward the phosphate binding site, and the Args away from that site (Fig. 4 and Movie S1). This rearrangement hinders the rebinding of the released phosphate and helps to drive the rotation forward. It is also associated with the extrusion toward the α_E-subunit of the loop region from residues 187–189 in the β_E-subunit (Fig. 4 and Movie S1). The movement of this loop is accompanied by a rotation of the nucleotide binding and C-terminal domains of the α_E-subunit (by 7° and 11°, respectively) relative to the nucleotide binding domain of the β_E-subunit, resulting in the opening of the $\alpha_E\beta_E$-interface in F_1-I_3-ThioP (Movie S2). In the absence of the rotation of the γ-subunit, this rotation of the C-terminal domain of the α_E-subunit would remove favorable packing (van der Waal's) interactions between the helix–turn–helix region of the α_E-subunit (residues 402–409) and the N-terminal α-helix of the γ-subunit (residues 18–30). However, in F_1-ThioP, these interactions have been retained by a 30° rotation of the γ-subunit (Fig. 5 and Movie S3). The interaction area between the γ- and α_E-subunits is 650 $Å^2$ in both F_1-ThioP and F_1-I_3-ThioP. However, if the γ-subunit in the F_1-I_3-ThioP complex is rotated artificially by 30° (modeled by using the α_E-subunit from F_1-I_3-ThioP and the γ-subunit from F_1-ThioP), the interaction area between the γ- and α_E-subunits is reduced to 407 $Å^2$. Thus, the binding energy gained from these new interactions, and from the formation of the salt bridge

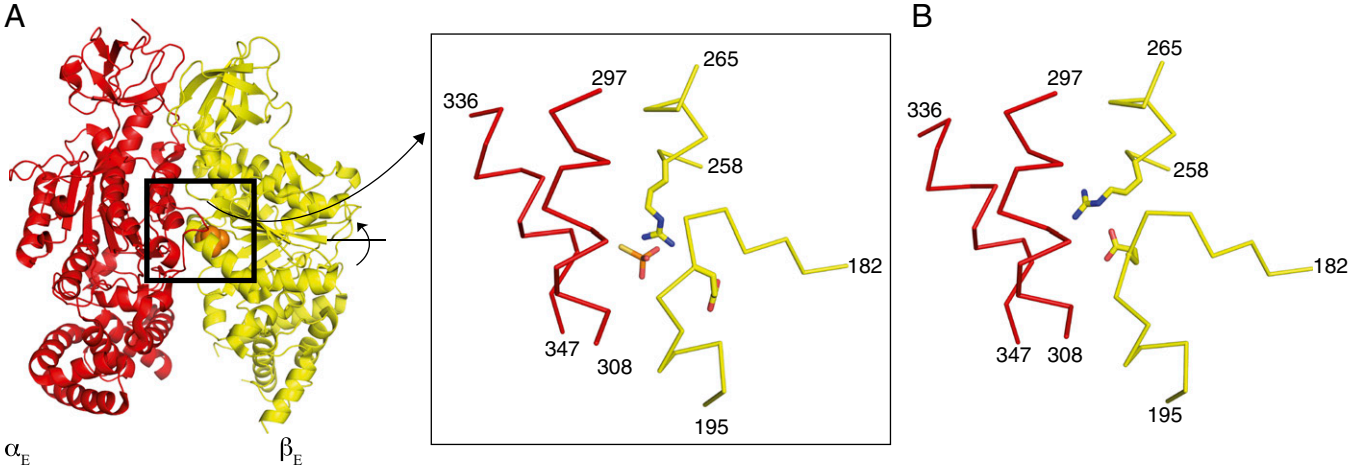

Fig. 4. Comparison of the structures of a loop region in the vicinity of the thiophosphate binding site in F_1-ThioP with the equivalent loop in F_1-I_3-ThioP. The loop, residues 187–189 of the β_E-subunit, contains residue β_E-E188. The α_E- and β_E-subunits and their structural elements are depicted in cartoon representation in red and yellow, respectively. (*A*) View toward the interface between the α_E- and β_E-subunits with the bound thiophosphate shown in orange and, in the box, an expanded view of the thiophosphate binding site. (*B*) Equivalent expanded view of the site in F_1-I_3-ThioP. In *A* and *B*, residues β_E-E188 and β_E-R260 are shown in stick representation, with oxygen and nitrogen atoms shown in red and blue, respectively.

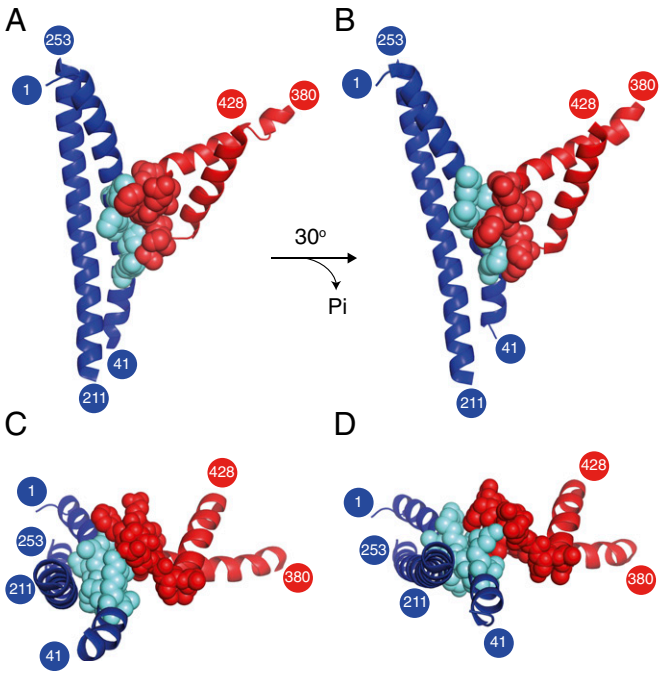

Fig. 5. Comparison of interactions between the γ-subunit and the α- and β-subunits in the F_1-ThioP and F_1-I_3-ThioP complexes. The blue α-helical regions are residues 1–41 and 211–253 of the γ-subunit. (*A*–*D*) F_1-ThioP and F_1-I_3-ThioP complexes, respectively; the residues in the γ- and α_E-subunits involved in these contacts are shown as light blue and red spheres, respectively. Views from the side (*A* and *B*) and from below (*C* and *D*) are depicted.

between β_E-E188 and β_E-R260 (Fig. 3), would help to compensate for the loss in binding energy associated with phosphate release.

Order of Release of the Products of Hydrolysis by F_1-ATPase. The order of the release of the products of ATP hydrolysis from F_1-ATPase is an unresolved issue. It has been proposed on the basis of single-molecule rotation experiments conducted on a bacterial F_1-ATPase that phosphate is released from the β_E-subunit after release of ADP (25, 26). Similar conclusions (27, 28) have been reached from molecular dynamics calculations based on bovine structural data (6) and bacterial rotational data (14). However, the structural data, derived almost entirely from eukaryotic enzymes, are ambiguous. The current structure of F_1-ThioP and the structure of "molecule" II of yeast F_1-ATPase (8) can be interpreted as being consistent with the release of ADP and the magnesium ion before the release of phosphate from the β_E-subunit. However, the structure, known as F_1-PH, of bovine F_1-ATPase crystallized in the presence of the magnesium ion chelator, phosphonate, contains an ADP molecule only, without an accompanying magnesium ion or phosphate, bound to a fully open β_E-subunit (11), suggesting that the release of both phosphate and magnesium (in an unspecified order) precedes the release of ADP. This order is consistent with the order of product release from other P-loop–containing nucleotide hydrolases, such as kinesin (29), G proteins (30), and myosin (31). In F_1-PH, the γ-subunit is rotated by 30.5° relative to the γ-subunit in F_1-ThioP, to a position similar to the position of the γ-subunit in F_1-I_3-ThioP. Therefore, it appears from this structure that ADP can remain bound to bovine F_1-ATPase after the release of phosphate. Further experiments are required to determine whether thiophosphate will bind to F_1-PH and whether ADP will bind to F_1-ThioP.

Another issue relating to product release from F_1-ATPase, where there are conflicting data, concerns the identity of the subunit from which phosphate is released. The data presented here, together with rotational studies on the human F_1-ATPase (23), show clearly that phosphate is released from the β_E-subunit. In an alternative catalytic mechanism, it is proposed that phosphate is released from the β_{DP}-subunit of the bacterial enzyme immediately following the hydrolysis of ATP and before the release of ADP (32). It is now apparent from rotational experiments that the catalytic cycles of human and bacterial F_1-ATPases differ significantly, as indeed they differ from the catalytic cycle of the related V-type ATPases, where there are three 120° steps per cycle with no observable substeps (33). These differences are likely to underlie the difficulties encountered hitherto in reconciling structural data from the bovine enzyme with rotational data determined on bacterial enzymes. The current experiments demonstrate that the structural and rotational data from the same or closely related species are compatible. The remaining challenge is to provide molecular explanations of the generation of the rest of the 120° step in the catalytic cycle.

Materials and Methods

Purification of Proteins. The bovine inhibitor protein I1-60His-K39A, comprising residues 1–60 of IF_1 with a C-terminal hexahistidine sequence and containing the mutation K39A, and bovine mitochondrial F_1-ATPase were purified as described previously (21).

Crystallization of the F_1-ThioP and F_1-I_3-ThioP Complexes. The growth of crystals, the dehydration procedure, and freezing conditions are described in *SI Materials and Methods*.

Data Collection and Processing. Diffraction data for the F_1-ThioP complex were collected to 3.1 Å on a Pilatus 6M detector (Dectris) on beamline I02 (fixed wavelength of 0.979 Å and beam size of 20 μm by 70 μm) at the Diamond Light Source (Harwell, UK). Diffraction data for the F_1–I_3–ThioP complex were collected to 3.3 Å on a Mar/Rayonix 3 × 3 mosaic 225 detector (Rayonix) on beamline ID23-2 (fixed wavelength of 0.87 Å and beam size of 8 μm by 8 μm) at the European Synchrotron Radiation Facility (Grenoble, France). Diffraction images were integrated with MOSFLM (34), and the data were reduced with AIMLESS (35). The structure of F_1-ThioP was solved by molecular replacement with PHASER (36) using the structure of bovine F_1-ATPase inhibited by azide (Protein Data Bank ID code 2CK3) without any of the bound nucleotides as the starting model. The structures were remodelled manually with Coot (37), and alternate rounds of rebuilding and refinement were carried out with REFMAC5 (38). The stereochemistry of each model was assessed with Coot and MolProbity (39). Images of the structures and electron density maps were generated with PyMOL (40). Surface areas of interaction between different subunits of F_1-ATPase were calculated with 'Protein interfaces, surfaces and assemblies' service PDBePISA (41).

Assessment of Positions of the γ-Subunit in Structures of Bovine F_1-ATPase. The azide-free ground state structure of bovine F_1-ATPase determined at 1.9 Å resolution was aligned with the structures of bovine F_1-ThioP, F_1-I1-60His, F_1-(I1-60His)$_2$, and F_1-(I1-60His K39A)$_3$ via their "crown" domains, consisting of residues 30–80 and 15–75 in the α- and β-subunits, respectively. In these structures, residues 22–32 of the γ-subunit interact directly with the C-terminal domains of the α- and β-subunits, and the position of this segment of the γ-subunit acts as a rigid body (Fig. S5) and should not be influenced by contacts in the crystal lattice between adjacent F_1-ATPase complexes, whereas the positions of the regions of the γ-subunit (residues 33–226), and the associated δ- and ε-subunits that, together, lie outside the $\alpha_3\beta_3$-domain, may be subject to such influences. Therefore, the rotations of residues 22–32 of the γ-subunit about the pseudo-threefold axis of the $\alpha_3\beta_3$-domain in the various aligned structures were measured relative to the position of the same segment in the azide-free ground state structure.

Generation of Movies. Movies were made with eMovie (42) and PyMOL. Morphs were generated with RigiMOL (40).

ACKNOWLEDGMENTS. We thank the staff at Beamline I02 at the Diamond Light Source (Harwell, UK) and Beamline ID23eh2 at the European Synchrotron Radiation Facility (Grenoble, France) for their help. This work was funded by the intramural program of the Medical Research Council (Grants U105663150 and U105184325 to J.E.W. and A.G.W.L., respectively).

1. Walker JE, Lutter R, Dupuis A, Runswick MJ (1991) Identification of the subunits of F_1F_o-ATPase from bovine heart mitochondria. *Biochemistry* 30(22):5369–5378.
2. Walker JE (2013) The ATP synthase: The understood, the uncertain and the unknown. *Biochem Soc Trans* 41(1):1–16.
3. Abrahams JP, Leslie AGW, Lutter R, Walker JE (1994) Structure at 2.8 Å resolution of F_1-ATPase from bovine heart mitochondria. *Nature* 370(6491):621–628.
4. Watt IN, Montgomery MG, Runswick MJ, Leslie AGW, Walker JE (2010) Bioenergetic cost of making an adenosine triphosphate molecule in animal mitochondria. *Proc Natl Acad Sci USA* 107(39):16823–16827.
5. Bowler MW, Montgomery MG, Leslie AGW, Walker JE (2006) How azide inhibits ATP hydrolysis by the F-ATPases. *Proc Natl Acad Sci USA* 103(23):8646–8649.
6. Bowler MW, Montgomery MG, Leslie AGW, Walker JE (2007) Ground state structure of F_1-ATPase from bovine heart mitochondria at 1.9 Å resolution. *J Biol Chem* 282(19): 14238–14242.
7. Gibbons C, Montgomery MG, Leslie AGW, Walker JE (2000) The structure of the central stalk in bovine F_1-ATPase at 2.4 Å resolution. *Nat Struct Biol* 7(11):1055–1061.
8. Kabaleeswaran V, Puri N, Walker JE, Leslie AGW, Mueller DM (2006) Novel features of the rotary catalytic mechanism revealed in the structure of yeast F_1 ATPase. *EMBO J* 25(22):5433–5442.
9. Kagawa R, Montgomery MG, Braig K, Leslie AGW, Walker JE (2004) The structure of bovine F_1-ATPase inhibited by ADP and beryllium fluoride. *EMBO J* 23(14):2734–2744.
10. Rees DM, Leslie AGW, Walker JE (2009) The structure of the membrane extrinsic region of bovine ATP synthase. *Proc Natl Acad Sci USA* 106(51):21597–21601.
11. Rees DM, Montgomery MG, Leslie AGW, Walker JE (2012) Structural evidence of a new catalytic intermediate in the pathway of ATP hydrolysis by F_1-ATPase from bovine heart mitochondria. *Proc Natl Acad Sci USA* 109(28):11139–11143.
12. Noji H, Yasuda R, Yoshida M, Kinosita K, Jr (1997) Direct observation of the rotation of F_1-ATPase. *Nature* 386(6622):299–302.
13. Nishizaka T, et al. (2004) Chemomechanical coupling in F_1-ATPase revealed by simultaneous observation of nucleotide kinetics and rotation. *Nat Struct Mol Biol* 11(2): 142–148.
14. Yasuda R, Noji H, Yoshida M, Kinosita K, Jr, Itoh H (2001) Resolution of distinct rotational substeps by submillisecond kinetic analysis of F_1-ATPase. *Nature* 410(6831): 898–904.
15. Menz RI, Walker JE, Leslie AGW (2001) Structure of bovine mitochondrial F_1-ATPase with nucleotide bound to all three catalytic sites: Implications for the mechanism of rotary catalysis. *Cell* 106(3):331–341.
16. Pullman ME, Monroy GC (1963) A soluble heat stable protein in mitochondria from bovine heart that inhibits ATP hydrolase activity. *J Biol Chem* 238:3762–3769.
17. Walker JE, Gay NJ, Powell SJ, Kostina M, Dyer MR (1987) ATP synthase from bovine mitochondria: Sequences of imported precursors of oligomycin sensitivity conferral protein, factor 6, and adenosinetriphosphatase inhibitor protein. *Biochemistry* 26(26): 8613–8619.
18. Cabezón E, Runswick MJ, Leslie AGW, Walker JE (2001) The structure of bovine IF_1, the regulatory subunit of mitochondrial F-ATPase. *EMBO J* 20(24):6990–6996.
19. Gordon-Smith DJ, et al. (2001) Solution structure of a C-terminal coiled-coil domain from bovine IF_1: The inhibitor protein of F_1 ATPase. *J Mol Biol* 308(2):325–339.
20. Cabezón E, Montgomery MG, Leslie AGW, Walker JE (2003) The structure of bovine F_1-ATPase in complex with its regulatory protein IF_1. *Nat Struct Biol* 10(9):744–750.
21. Bason JV, Montgomery MG, Leslie AGW, Walker JE (2014) Pathway of binding of the intrinsically disordered mitochondrial inhibitor protein to F_1-ATPase. *Proc Natl Acad Sci USA* 111(31):11305–11310.
22. Gledhill JR, Montgomery MG, Leslie AGW, Walker JE (2007) How the regulatory protein, IF_1, inhibits F_1-ATPase from bovine mitochondria. *Proc Natl Acad Sci USA* 104(40):15671–15676.
23. Suzuki T, Tanaka K, Wakabayashi C, Saita E, Yoshida M (2014) Chemomechanical coupling of human mitochondrial F_1-ATPase motor. *Nat Chem Biol* 10(11):930–936.
24. Walker JE, Saraste M, Runswick MJ, Gay NJ (1982) Distantly related sequences in the alpha- and beta-subunits of ATP synthase, myosin, kinases and other ATP-requiring enzymes and a common nucleotide binding fold. *EMBO J* 1(8):945–951.
25. Watanabe R, Iino R, Noji H (2010) Phosphate release in F_1-ATPase catalytic cycle follows ADP release. *Nat Chem Biol* 6(11):814–820.
26. Watanabe R, Noji H (2014) Timing of inorganic phosphate release modulates the catalytic activity of ATP-driven rotary motor protein. *Nat Commun* 5:3486.
27. Nam K, Pu J, Karplus M (2014) Trapping the ATP binding state leads to a detailed understanding of the F_1-ATPase mechanism. *Proc Natl Acad Sci USA* 111(50): 17851–17856.
28. Okazaki K, Hummer G (2013) Phosphate release coupled to rotary motion of F_1-ATPase. *Proc Natl Acad Sci USA* 110(41):16468–16473.
29. Milic B, Andreasson JO, Hancock WO, Block SM (2014) Kinesin processivity is gated by phosphate release. *Proc Natl Acad Sci USA* 111(39):14136–14140.
30. Wittinghofer A, Vetter IR (2011) Structure-function relationships of the G domain, a canonical switch motif. *Annu Rev Biochem* 80:943–971.
31. Gulick AM, Rayment I (1997) Structural studies on myosin II: Communication between distant protein domains. *BioEssays* 19(7):561–569.
32. Junge W, Sielaff H, Engelbrecht S (2009) Torque generation and elastic power transmission in the rotary F_OF_1-ATPase. *Nature* 459(7245):364–370.
33. Minagawa Y, et al. (2013) Basic properties of rotary dynamics of the molecular motor *Enterococcus hirae* V_1-ATPase. *J Biol Chem* 288(45):32700–32707.
34. Leslie AGW (2006) The integration of macromolecular diffraction data. *Acta Crystallogr D Biol Crystallogr* 62(Pt 1):48–57.
35. Evans PR, Murshudov GN (2013) How good are my data and what is the resolution? *Acta Crystallogr D Biol Crystallogr* 69(Pt 7):1204–1214.
36. McCoy AJ, et al. (2007) Phaser crystallographic software. *J Appl Cryst* 40(Pt 4):658–674.
37. Emsley P, Lohkamp B, Scott WG, Cowtan K (2010) Features and development of Coot. *Acta Crystallogr D Biol Crystallogr* 66(Pt 4):486–501.
38. Murshudov GN, et al. (2011) REFMAC5 for the refinement of macromolecular crystal structures. *Acta Crystallogr D Biol Crystallogr* 67(Pt 4):355–367.
39. Chen VB, et al. (2010) MolProbity: All-atom structure validation for macromolecular crystallography. *Acta Crystallogr D Biol Crystallogr* 66(Pt 1):12–21.
40. DeLano WL, The PyMOL Molecular Graphics System (Schrödinger, LLC, New York), Version 1.7.
41. Krissinel E, Henrick K (2007) Inference of macromolecular assemblies from crystalline state. *J Mol Biol* 372(3):774–797.
42. Hodis E, Schreiber G, Rother K, Sussman JL (2007) eMovie: A storyboard-based tool for making molecular movies. *Trends Biochem Sci* 32(5):199–204.